JOURNAL OF BACTERIOLOGY, June 1981, p. 1135-1150
0021-9193/81/061135-16$02.00/0

Vol. 146, No. 3

Periodic Surface Array in *Caulobacter crescentus*: Fine Structure and Chemical Analysis

JOHN SMIT,[1] DAVID A. GRANO,[2] ROBERT M. GLAESER,[2] AND NINA AGABIAN[1]*

Department of Biochemistry SJ-70, University of Washington, Seattle, Washington 98195,[1] and Department of Biophysics and Medical Physics and Donner Laboratory, University of California, Berkeley, California 94720[2]

Received 19 January 1981/Accepted 23 March 1981

A periodic array structure on the cell surface of *Caulobacter crescentus* CB15 was revealed by electron microscopy of the cell envelope, using negative staining, thin-sectioning, and freeze-etching. This structural layer has been isolated from liquid cultures, in which large pieces of the two-dimensional array are shed by cells grown to high density. Often areas of intact array corresponding to the entire cell surface could be found. The hexagonally arranged structure was highly ordered and had an unusual degree of complexity, as determined by optical diffraction and computer processing of micrographs of negatively stained, isolated surface array. Filtered, reconstructed images were obtained from both normal and low-electron-dose micrographs demonstrating resolutions of 2.9 and 2.5 nm, respectively. Comparison by optical diffraction and image filtering of micrographs recorded by using either normal or minimal beam exposure techniques suggested that the lower-resolution features of the image are very stable to electron exposure. Gel electrophoresis indicated that isolated array preparations contain a number of polypeptides. It appears likely that more than one of these proteins are structural components of the array, in contrast to a single protein found in many bacterial surface arrays. The *Caulobacter* surface array is also unusual in that the repeated units are widely spaced with no apparent direct connection. Computer spatial averaging provided information about the shape and complexity of the connecting elements, and this was compared with some additional electron microscopic evidence of linking structures. Thin-sectioning studies confirmed the image features seen by other techniques, but the addition of tannic acid in the fixation procedure was required to visualize the structure. A comparison of these results with our current knowledge of the *Caulobacter* cell envelope suggests interesting questions about the biogenesis of this membrane structure and its involvement in the cell development process of this organism.

The existence of bacterial surface layers composed of regularly aligned subunits capable of self-assembly has been recognized for some time (14, 31). The number of genera which are known to exhibit these layers has grown in recent years, apparently due to careful reexamination of various bacteria and an increasing interest in such structures (31). Regular surface layers are found in both gram-positive and gram-negative bacteria, and despite major differences in underlying cell wall structures, their gross appearances are surprisingly similar. The subunits in the arrays are usually hexagonally or tetragonally arranged (31) and sometimes form multiple layers on an organism (8, 40).

The molecular composition of these surface layers usually consists of a single species of protein. This compositional simplicity is often reflected in the electron microscopic appearance of the layer: the subunits make direct contact with one another, obviating the requirement for additional interconnecting elements.

A significant proportion of a cell's synthetic activity is expended in the production of these arrays, suggesting an important role, yet in most cases their function remains unknown. Some bacterial species with surface layers are more resistant to peptidoglycan hydrolases or proteolytic enzymes than their unadorned counterparts (21, 32), and for this reason, a barrier role for these layers has often been suggested. In *Spirillum serpens*, a surface layer appears to prevent attack by parasitic *Bdellovibrio* cells (F. L. A. Buckmire, Bacteriol. Proc., p. 43, 1971). In several *Clostridium* species, the surface layer prevents the release of internal toxins (31). Enzymatic activities and attachment functions residing in these layers have also been reported

(26, 38). Thus, whereas many surface layers share a similar appearance, the environmental pressures which select for these structures seem to arise from a variety of sources.

The interest in these bacterial surface layers also extends to the general study of membrane structure and biogenesis. Since the excreted proteins remain associated with the cell and can be visually assayed, the surface arrays may offer tractable systems to examine mechanisms of protein secretion, insertion into membranes, and membrane formation and maintenance.

We have discovered a surface layer of unusual complexity in one strain of *Caulobacter crescentus*. We report here the isolation and characterization of this membrane structure and several properties that make it unusually amenable to in-depth analysis. Morphogenesis and development in *C. crescentus* are largely expressed in the membranes of the cell (2, 26), and therefore an understanding of all aspects of these membranes is important. Most other bacterial systems in which surface arrays have been characterized have not been extensively characterized from genetic and biochemical standpoints. In contrast, *C. crescentus* is the subject of multiple studies at these and other molecular levels (27). Thus, the combination of array complexity and system knowledge presents an ideal circumstance to study structure-function relationships and mechanisms involved in the biogenesis of a regular surface structure.

MATERIALS AND METHODS

Bacterial strains and growth conditions. *C. crescentus* CB15, CB13, and 15NY106 were used. 15NY106 was provided by Jeanne Poindexter and is an "abscission" mutant of CB15 characterized by a tendency to shed stalks, possibly due to an aberrant placement of a division plane (23). For the production of surface array material, cells were grown in modifications of HIGG minimal medium (23). M_1HIGG contains 5 mM imidazole hydrochloride (pH 7.0), 10 mM potassium phosphate, 1% modified Hutner mineral base (12), 0.3% glucose, 0.3% sodium glutamate (pH 7.0), and 0.05% NH_4Cl; M_3HIGG is identical to M_1HIGG except that the potassium phosphate level is reduced to 2 mM. Cells were also grown in modified peptone-yeast extract (4, 22) or glucose minimal medium (28) as indicated. Liquid cultures were incubated at 30°C on a rotary shaker.

Isolation of the regular surface array. For most experiments strain 15NY106 was used because, as compared with other strains, this strain appears to slough off a greater amount of intact surface array which is largely free of sheets of underlying membrane material. Typically, 1 liter of cells was grown in M_3HIGG medium to mid-stationary phase (optical density at 660 nm, 3 to 4). The culture was centrifuged three times at 6,000 × *g* for 30 min, with the cell pellet being discarded each time. The supernatant was centrifuged at 15,000 × *g* for 30 min, and the resulting pellet was suspended in 25 ml of 1 mM $MgCl_2$–1 mM $CaCl_2$–3 mM NaN_3; residual cells were removed by centrifugation at 5,000 × *g* for 10 min. This final supernatant fluid was centrifuged at 15,000 × *g* for 10 min, and the pellet was suspended in 2 to 3 ml of the $MgCl_2$-$CaCl_2$ solution and stored at 4°C.

For some experiments, strain CB15 was grown in M_1HIGG medium and the array material produced was isolated in the same way.

Protein analysis. The proteins in the array were examined by sodium dodecyl sulfate-polyacrylamide gel electrophoresis by the method of Laemmli (18), modified as previously described (41). For most experiments, a gradient of 10 to 15% acrylamide was used. For quantitation, the slab gels were dried onto clear cellophane sheets (Bio-Rad) and were scanned with a Joyce-Loebl recording microdensitometer MKIIC equipped with electronic peak integration.

Electron microscopy. For freeze-etching, cells were grown in glucose minimal or peptone-yeast extract medium, centrifuged at 12,000 × *g* for 10 min, and washed by suspension and centrifugation in 0.02 M potassium phosphate buffer (pH 7.0). The cell pellet was suspended in buffer containing 1.5% glutaraldehyde and fixed for 30 min at room temperature. The fixed cells were washed twice in water and resuspended in a small amount of water. Portions of this preparation were frozen on cardboard disks in the liquid phase of Freon 22, which was held partially solidified by liquid nitrogen.

Fracturing was accomplished in a Balzars 301 apparatus, using standard methods (34). Etching was done at a stage temperature of −96°C, followed by platinum shadowing (controlled by a quartz crystal monitor) and carbon coating. The resulting replicas were cleaned by treatment with methanol followed by sodium hypochlorite (33) and several changes of water. The replicas were mounted on uncoated copper grids.

Negative staining was performed on 500-mesh copper grids, using a Formvar support film stabilized by vacuum deposition of carbon and rendered hydrophilic by vacuum deposition of a thin layer of silicon monoxide (37). Grids were floated on a droplet of the array mixture and moved into another droplet of negative stain, and excess fluid was removed with filter paper.

In the course of this study, the staining properties of a variety of negative stains, including 2% ammonium molybdate (pH 7.5 with NH_4OH), 1% uranyl acetate (pH 4.5), 2% uranyl oxalate (pH 7.0), 1% potassium phosphotungstate (pH 7.0), 2% phosphomolybdic acid (pH 7.5), 2% sodium tungstate (pH 7.5 with NaOH), 2% sodium silicotungstate (pH 8.0 with HCl), and 2% ammonium tungstate (pH 7.5 with NH_4OH), were examined. The two-step technique of Horne and Ronchetti (16), using uranyl acetate and ammonium molybdate, was also applied to this system.

For ultrathin-section analysis, mid-logarithmic-phase cells were centrifuged at 12,000 × *g* for 10 min and suspended in 5% acrolein–1% glutaraldehyde–5 mM $CaCl_2$–0.1 M sodium cacodylate (pH 7.0) with or without 2% tannic acid (Sigma Chemical Co.). After incubation at room temperature for 2 to 4 h, the cells were centrifuged and washed in 0.1 M sodium cacodylate (pH 7.0) buffer containing 5 mM $CaCl_2$. The

cell pellet was suspended in an equal volume of 2.5% agarose in cacodylate buffer held at 48°C. The resulting mixture was chilled, cut into pieces, and washed twice with buffer.

The cells were then fixed in 1% OsO_4 in cacodylate buffer containing 5 mM $CaCl_2$ and 500 μg of ruthenium red per ml (the latter was added just before use). After fixation, the preparation was washed once with buffer and twice with water and treated with 0.5% uranyl acetate for 1.5 h, followed by two additional washes with water. The preparation was then directly dehydrated with acidified dimethoxypropane (20) and embedded in Spurr resin.

Ultrathin sections were cut with an LKB Huxley ultramicrotome, mounted on copper grids without support films, and stained with uranyl acetate and lead citrate.

When negatively stained specimens were examined under conditions of minimal electron irradiation, the basic technique of Williams and Fisher (42) was used. A JEOL 100B microscope, operating at 60 kV, was used; exposures were recorded on Kodak 4463 film developed for "maximum" speed. For all other electron microscopy, a Phillips EM201 microscope was used, operated at 60 or 80 kV. Micrographs were recorded on 4463 film, exposed, and developed for "medium" speed.

A precise determination of the center-to-center spacing of the array elements was made by adding uniform-diameter latex spheres (0.109 μm, standard deviation, 2.7 nm; Pelco) to a standard negatively stained preparation. As an additional standard, magnification was calibrated by using a grating replica (54,800 lines per in.; ca. 21,600 lines per cm).

Image processing. Micrographs of the negatively stained periodic surface array were screened for further computer processing by optical diffraction methods to select those images demonstrating the highest preservation of periodicity. Images thus selected were scanned on a Perkin-Elmer PDS 1010A scanning microdensitometer, using 30-, 50-, or 100-μm scanning rasters, depending on micrograph magnification, and were computer processed by using the Lawrence Berkeley Laboratory image processing system. Discrete Fourier transforms of image areas about 280 nm on a side were calculated for the high-dose images, and areas 570 nm on a side were used from the minimal-beam images. Structure factors and phases were retrieved from these Fourier transforms. No corrections were made to the amplitudes to account for the effect of the contrast-transfer function. All of the diffraction orders fell within the first contrast-transfer zone, so phase corrections were unnecessary. The phase origins of the transforms were refined assuming a minimal planar symmetry of p6. Filtrations were done using both actual and symmetrized data. Data from the high-dose images were combined into one set by a linear least-squares scaling of amplitudes, as were data from the minimal-beam images. Final filtrations were done from these sets.

RESULTS

Negative staining analysis. There was little indication of the presence of a periodic surface structure in intact negatively stained CB15 cells due to the density contributed by the thickness of the cell. The periodic array can, however, be seen on ruptured cells where most of the underlying cell contents have been extruded (Fig. 1). The array network encompassed the entire swarmer or stalked cell, including the stalk region. Interestingly, it was only found in strain CB15 and not in the other commonly used *C. crescentus* strain, CB13.

In cultures grown to high density, enough sloughed-off intact surface array material accumulated to permit its isolation by differential centrifugation. *C. crescentus* 15NY106 was primarily used for these preparations because large pieces of surface array, often about 1 μm in diameter, were shed by this mutant (Fig. 2). The parent and other strains did not slough off as much of the material, and membrane material remained attached to the isolated array as sheets or large vesicles (Fig. 3), making it more difficult to see the fine structure details by negative staining. The cells were grown in modified HIGG media, which supported the growth of cells to very high densities (about 10^{10} cells per ml), thereby increasing the yield of sloughed-off array.

The isolated surface array was a very stable complex. Excellent optical diffraction patterns could be obtained from micrographs taken many months after the complex was isolated. The addition of Mg^{2+} and Ca^{2+} ions during the isolation and storage seemed to enhance that stability, and therefore they were included at all times.

A variety of negative stains were evaluated for suitability in staining the isolated array. The commonly used stains, uranyl acetate and potassium phosphotungstate, completely disrupted the array, leaving almost no indication that a preparation contained the structure. Uranyl oxalate yielded an acceptable image, suggesting that uranyl acetate may be unsuitable because of its low pH. No rules could be deduced from staining with tungsten compounds; sodium silicotungstate destroyed the array, whereas ammonium tungstate provided adequate staining and sodium tungstate yielded very good results. These latter stains were all used at approximately neutral pH. Phosphomolybdate also stained the array without destruction, but the best stain in terms of contrast, penetrability, and reproducibility was ammonium molybdate. Accordingly, this stain was used for most of the work described herein.

The main feature of the array when viewed by the negative staining procedures was distinct, circular rings arranged at precise intervals in a hexagonal array (Fig. 2). Regular, geometric

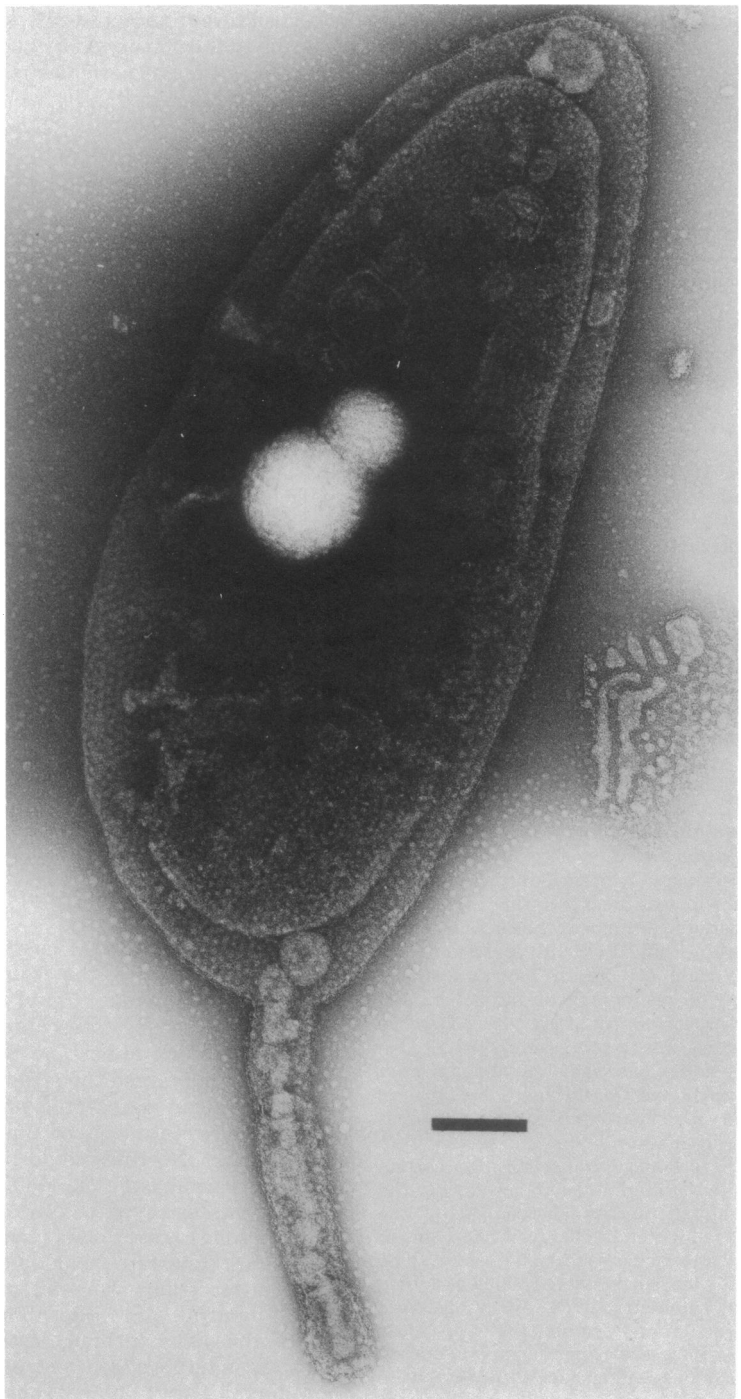

FIG. 1. *Negative-stain electron microscopy of a ruptured CB15 stalked cell, which was occasionally found in cell cultures. The absence of cytoplasmic contents allows visualization of a periodic structure on the cell surface. Note that the surface layer covers the entire cell, including the stalk. Negatively stained with 2% ammonium molybdate. The bar in this and subsequent micrographs indicates 0.2 μm, unless otherwise noted.*

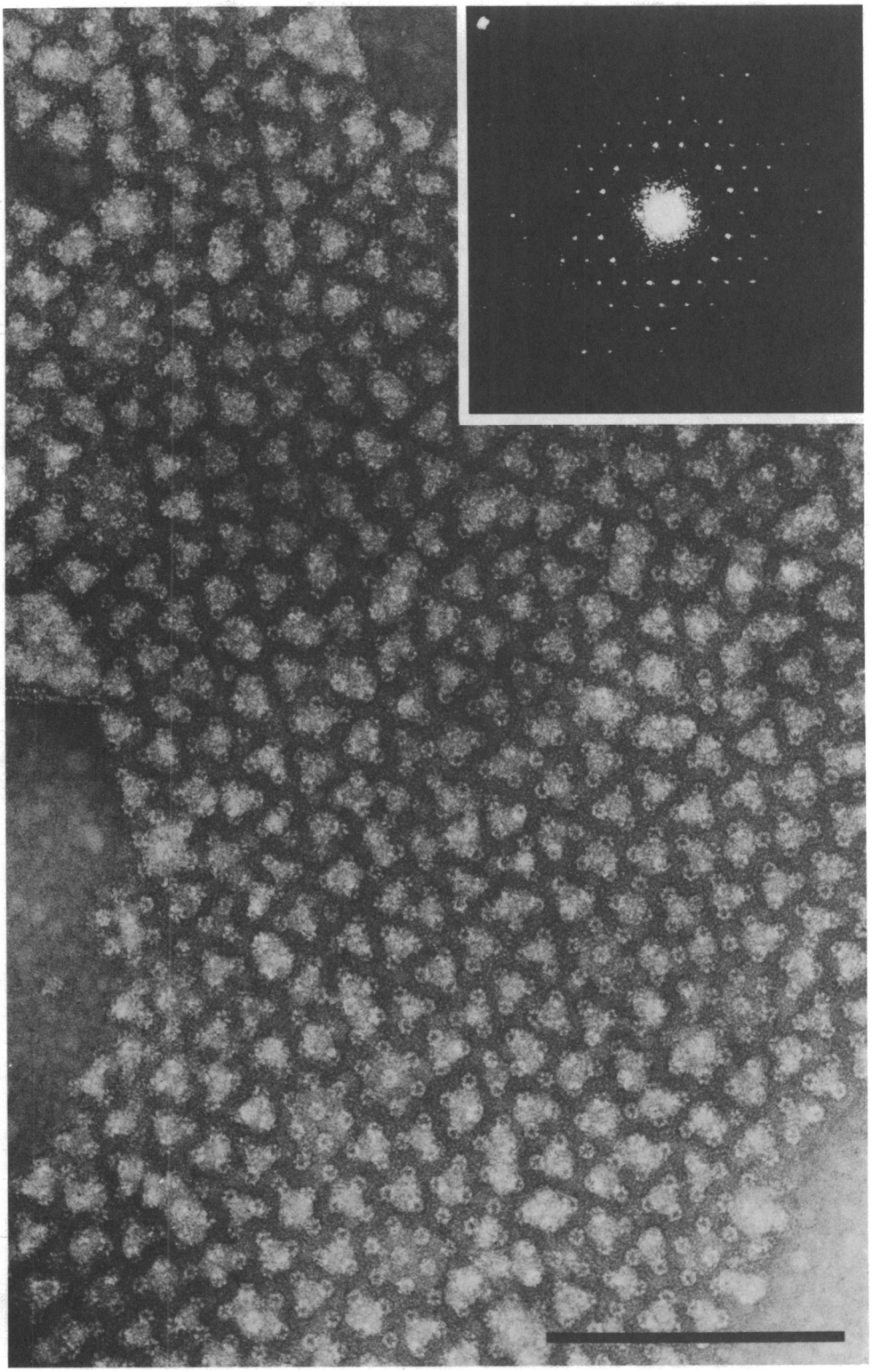

FIG. 2. *Isolated surface array from strain 15NY106 as seen by negative staining with ammonium molybdate. This micrograph was recorded by normal (high-electron-dose) electron microscopy. The highly ordered structures are the small rings. The amorphous stain-excluding vesicles are somewhat randomly interspersed in the isolated membrane-free array and do not contribute to the diffraction pattern. Inset shows the optical diffraction pattern obtained from this micrograph, indicating the regularity of the repeated structures. Compare this diffraction pattern with the one for the low-electron-dose image in Fig. 7.*

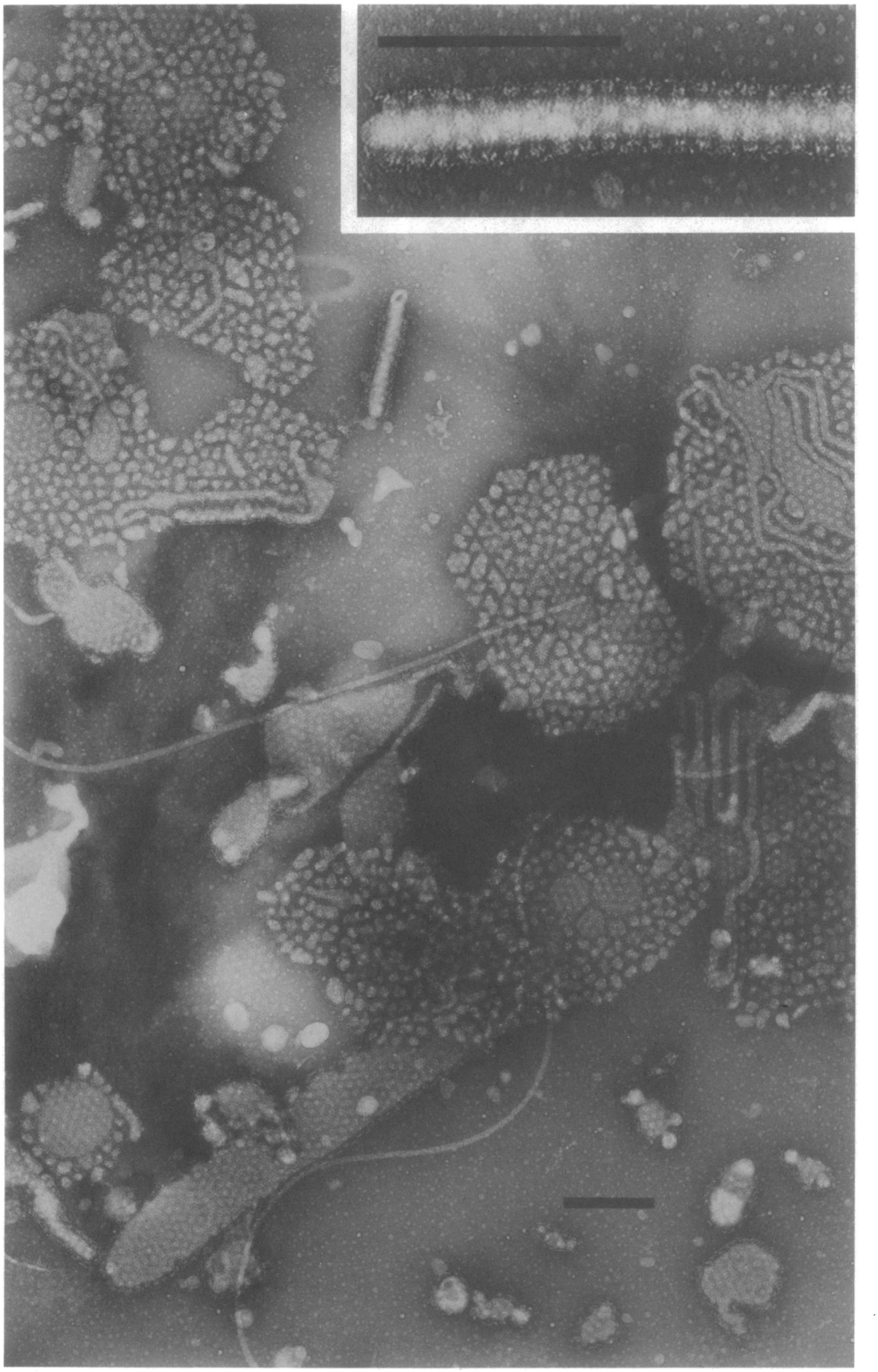

FIG. 3. *Isolated surface array from the parent strain CB15. This lower-magnification micrograph shows the variety of structures seen when a large amount of the relatively intact, underlying membrane remains attached. Various forms of membrane, including sheets, tube structures, and small vesicles, can be seen. A few flagella are also visible. The inset shows a higher-magnification view of a tube structure, demonstrating a side view of the attached surface array. The height of the repeating elements can be judged, and some indication of the connecting structures is seen. The material in both images was negatively stained with ammonium molybdate.*

spacing of these units, extending for large distances, was commonly observed. The rings are about 12.0 nm in diameter, with a center-to-center spacing of 23.5 nm. Little information about the components connecting the rings or the three-dimensional aspects of the structure of these subunits was obtained by viewing in the normal fashion (i.e., perpendicular to the array plane). However, when the isolated array remained attached to membrane material, as was frequently the case in parent strain CB15, elongated vesicles were often formed. At the edge of these vesicular structures, the array could be examined in side view (inset, Fig. 3). From this perspective, the circular rings are seen as short tubular or rodlike structures attached to the surface of the membrane material. These rods are about 11.0 nm tall. In this view, one can also see some evidence of components at the outermost surface which seem to connect the rings and which are presumably involved in maintaining their precise spacing. It is difficult to resolve the nature of the connections between the rings, but it is clear from the negative staining and thin-section analysis (see below) that the connection does occur at the outermost surface.

Occasionally, at the edge of an array patch and with optimal thickness of the negative stain, rodlike or fibrous structures were visible at the torn edge of the patch (Fig. 4). These rods appeared to be semirigid; they had a uniform degree of curvature, and measurements indicated a uniform tip-to-tip distance of 50.0 nm. The regularity of these structures was quite striking, and their close association with array patches suggests that they are contained in the isolated complex. However, we are unable to say whether they were derived from a structural component of the periodic surface layer or whether they represent an additional component sloughed off the cell along with the array.

The array material isolated from 15NY106 also contained numerous pieces of stain-excluding material, which seemed to be arranged in a quasi-regular pattern relative to the true (periodic) lattice of ringlike subunits. The stain-excluding pieces of material tended to be triangular in shape, with the vertices of the triangles apparently making contact with the ringlike subunits (Fig. 2). This material most likely is outer membrane, which formed vesicles after removal from the cell surface. This interpretation is supported by thin-section microscopy of array material, which revealed bilayer vesicle structures 20 to 30 nm in diameter (data not shown). In contrast, arrays isolated from CB15 contained many large membrane sheets or vesicles and appeared qualitatively to have more outer membrane attached (Fig. 3). The apparent difference in the appearance of the membrane layers between these two cells types is not understood; however, this observation may indicate a subtle

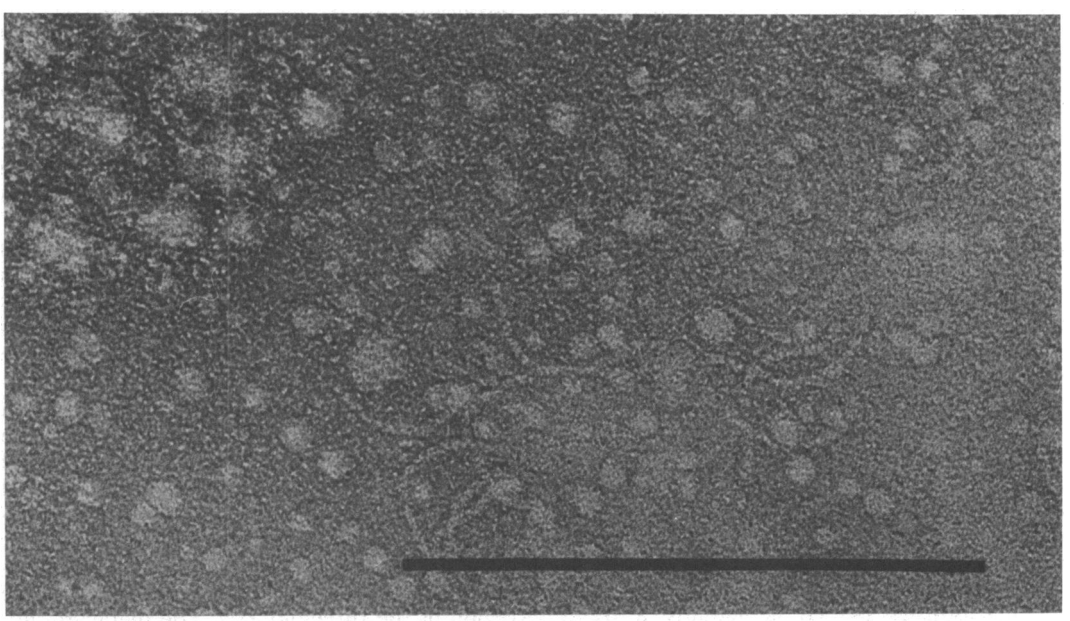

FIG. 4. *Elements seen at the edge of an isolated array patch. They have a uniform curvature, resulting in a tip-to-tip distance of 50.0 nm, and a diameter of 2.5 to 3.0 nm. At the upper left is a small portion of the nearby array patch. At the lower left is a segment of a flagellar filament, included for size comparison. Negatively stained with ammonium molybdate.*

alteration in the association of the array structures with the outer membrane or in the physical properties of the outer membrane itself.

Thin-section analysis of *C. crescentus*. Conventional cell preparations for thin-section analysis do not indicate the presence of a surface structure exterior to the outer membrane in *C. crescentus* (24). Although the addition of ruthenium red to the OsO_4 fixative significantly improved the contrast of the inner and outer membranes and of the well-defined peptidoglycan layer, there was still no indication of the surface array (Fig. 5a). However, addition of tannic acid to the aldehyde fixation step dramatically revealed tbe presence of the periodic structure (Fig. 5b) in detail comparable to that seen by negative staining (Fig. 3). Available evidence on the mechanism of action of tannic acid suggests that it functions by binding to the array, rendering it stainable with OsO_4 (29). It is possible that the binding of tannic acid also prevents loss of the surface array during fixation. It was not possible to further resolve the cross-sectional appearance of the surface layer; even in thin sections (i.e., 60 to 80 nm), two or three rows of array elements are contained within the plastic section, and their superposition may contribute to the inability to discern precise structural details.

Cross-sectional analysis gave no indication of additional wall layers between the outer membrane and the surface array structure. Therefore, we assume provisionally that the membrane material adherent to the array preparations only represents portions of the outer membrane shed along with surface array structures. This is in contrast to the additional "backing" layer proposed for the surface arrays of *Spirillum metamorphum* (6), *S. serpens* (9, 11), and *Micrococcus radiodurans*, a gram-positive organism (5).

Freeze-etching studies. Freeze-etching analysis of CB15 also revealed a periodic structure on the surface (Fig. 6), but there was poor long-range order. Little fine structure of the array could be resolved by this method, and alterations in metal shadowing methods did not improve the appearance. Resolution of the surface array by this technique might be obscured by a meshwork of interconnecting elements which prevents sufficient relief of the ring structures. Alternatively, penetration of the surface array by outer membrane polysaccharide chains or a thin layer of capsular material may be obscuring the array. Finally, distortion of surface features might have occurred during the freeze-etching process (which is actually a freeze-drying), although this technique has been used to obtain excellent images of other bacterial surface arrays (31).

Optical diffraction and computer Fourier analysis. Images obtained from normal microscopy (high electron dose) and minimal beam exposure microscopy (low electron dose) were selected on the basis of their optical diffraction patterns and analyzed further by computer processing. The optical diffraction patterns demonstrated that structural periodicity was maintained at least to the seventh order (Fig. 2) in the case of the high-dose images and to the ninth order in optimal-low-dose images (Fig. 7).

A general analysis of the optical diffraction patterns of the array indicate a very high degree of structural regularity. To generate such a pattern, the basic structural units must be accurately aligned with respect to one another. The amorphous islands of material (probably outer membrane vesicles, as discussed above) were not retained in the image, after the application of the techniques of spatial averaging, because they are not arranged in a regular way over the lattice.

The images that were used for computer averaging revealed a trigonal periodic planar lattice ($|a^*| = |b^*|$ to within 1%; the included angle equal to 60°, within 1°). An assumption of p3 planar symmetry was made and the coordinate origin was moved onto the presumed threefold axis at the center of the ringlike subunit. In both sets of images, the resulting phases were quite close to 0 or 180°, and therefore the phases were subsequently refined to p6 symmetry. For the high-dose micrographs, the average absolute deviation from p6 phase symmetry was 36° out to the resolution limit of the micrographs (2.9 nm). For the minimal-beam images, this deviation was only 27° out to 2.5-nm resolution. These values of phase error are typical in image-processing work with negatively stained specimens. There was no evidence of p6m symmetry, since there was marked asymmetry of the hk, kh terms.

Comparison between optical diffractograms recorded from normally exposed micrographs and those from minimal beam exposure conditions showed a definite improvement of resolution in the low-dose images. Consistently higher diffraction orders were recorded from minimal-exposure micrographs, and some alterations in intensities of reflections of lower orders were also noted (Fig. 2 and 7). Yet the high-dose and minimal-beam filtered images demonstrated basic similarities. There were six discrete subunits within each ring, and a fainter, triangular density, perhaps corresponding to the interconnecting elements of the lattice, was found in the region of the threefold axis. The higher-resolution, minimal-beam filtered image showed a somewhat elliptical, slewed shape of the six subunits within the rings (Fig. 8). The subunits had

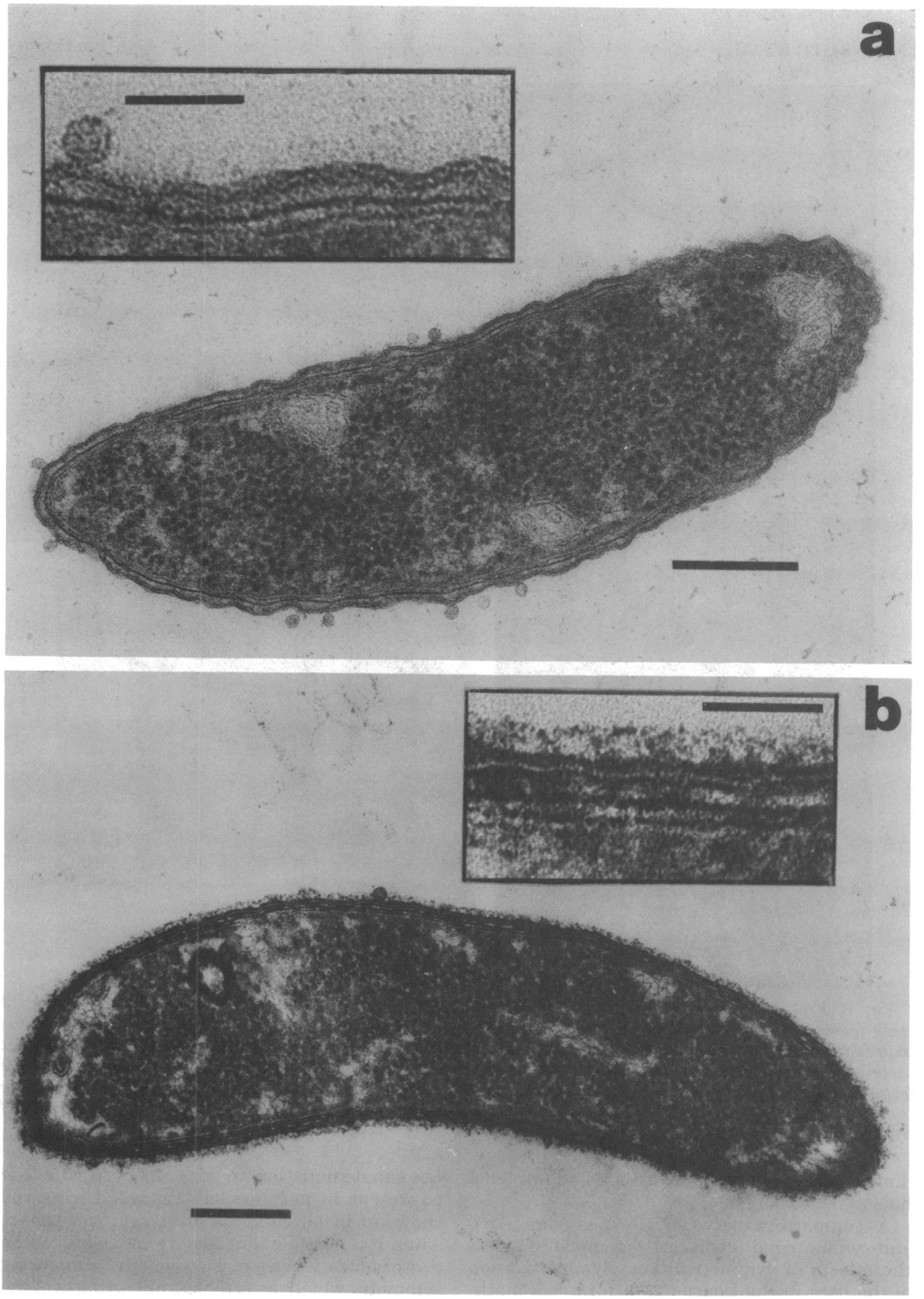

FIG. 5. *Thin-section electron microscopy of strain CB15 showing the effects of the addition of tannic acid to the fixation protocol. (a) Cells were fixed and stained as described in the text with no added tannic acid. The membranes and cytoplasmic contents are well preserved and have good contrast, yet no additional layers are evident. (b) This cell was fixed in the same way as in (a) except tannic acid was included in the fixation procedure. A surface structure comparable to that seen by negative staining is seen. The insets for both figures are higher magnifications of cell wall regions of the same micrographs. Inset bars indicate 0.05 μm.*

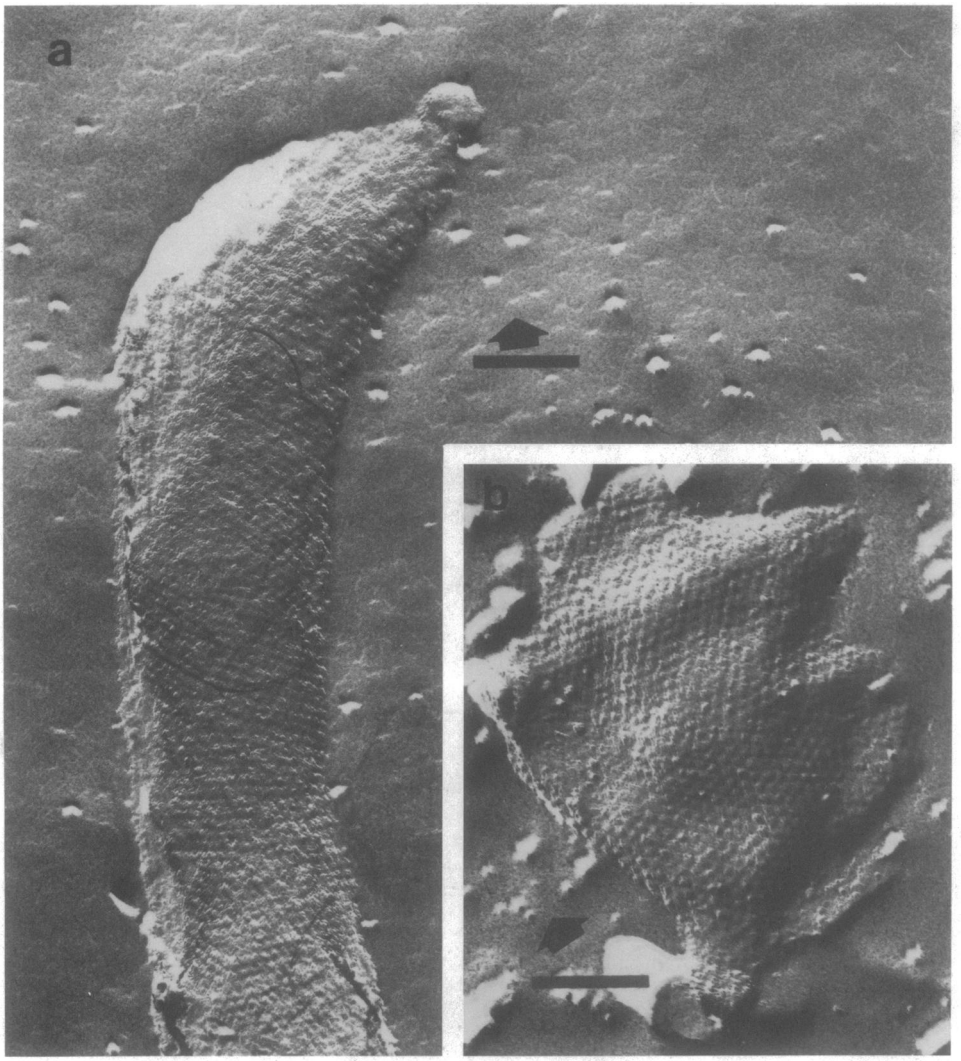

FIG. 6. *Freeze-etching of strain CB15. (a) This is an early stalk cell, apparently showing the first signs of stalk formation. In this typical view, there are indications of a periodic structure on the surface, but the impression of precise, long-range order was not seen. (b) This image of a portion of a cell surface shows that occasionally good order of the repeated structures can be obtained. It is likely that the resolution of the technique, which includes such considerations as the amount of metal shadow necessary for adequate contrast, prevents visualizing individual elements of the six-member rings. Arrows indicate the direction of shadowing.*

dimensions of about 4.5 by 2.5 nm and formed a hole of 3.0 to 3.5 nm.

A comparison between the unsymmetrized and symmetrized filtrations was made to assess the effects of symmetrization. Symmetrization of the data in the Fourier transform is a mathematical procedure for averaging the images of symmetry-related subunits. Viewed in this way, symmetrization may be expected to reinforce true features of the structure, while reducing or "averaging out" random features. As a caution, one should note that any prominent feature that is present in just one subunit will necessarily show up in all subunits after symmetrization. Thus, it is possible that the averaging procedure can produce images of pleasing and convincing symmetry which nevertheless are artifacts of the symmetrization operation. However, all of the basic features found in the symmetrized version were present in the unsymmetrized filtration (Fig. 8).

It is presumed that the minimal exposure

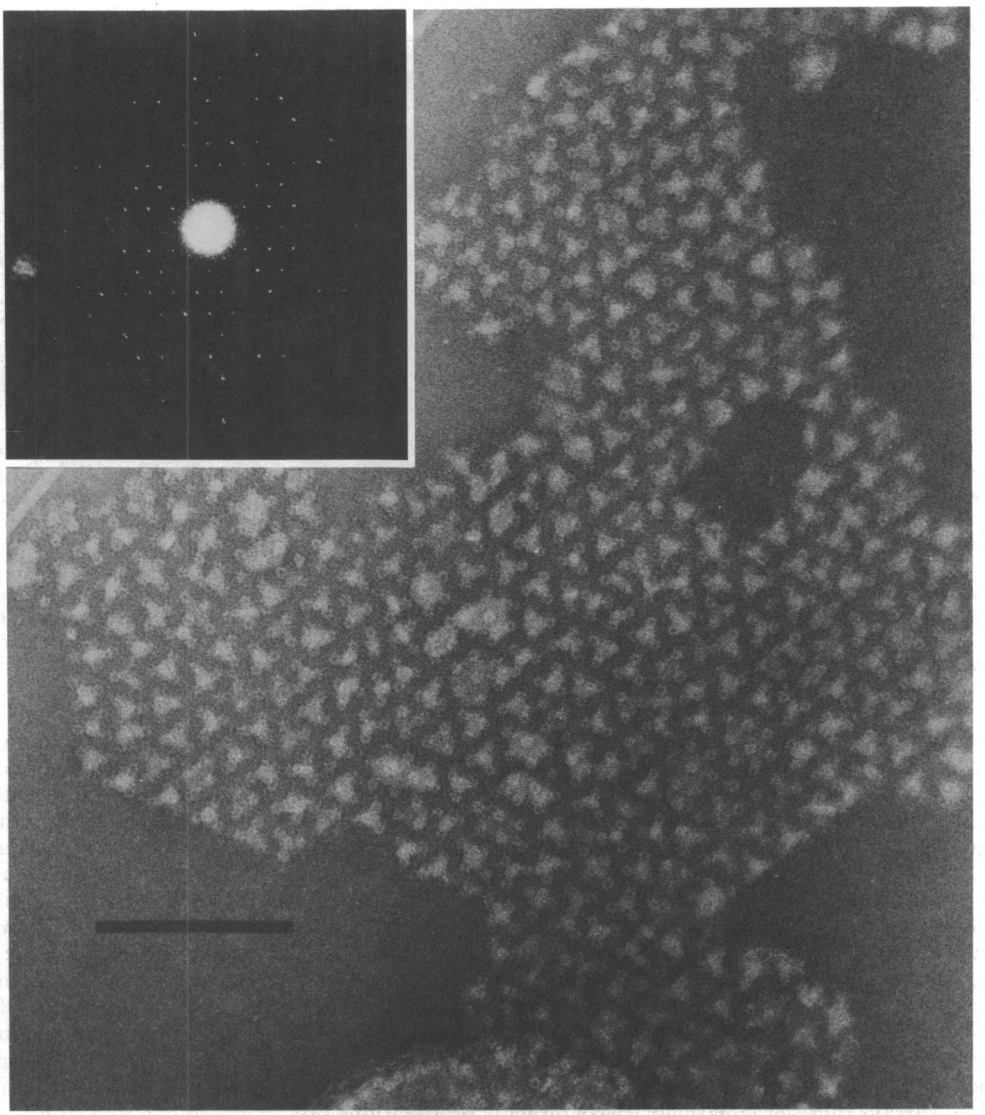

FIG. 7. *Isolation surface array from strain 15NY106 recorded by minimum beam exposure techniques. Although detail is not seen as clearly as in normal exposures, reduced effects of electron exposure resulted in a superior optical diffraction pattern. Inset demonstrates the optical diffraction pattern recorded from this image. When compared to an optical diffractogram of a normal exposure (Fig. 2), higher diffraction orders, smaller diffraction spots, and more variable spot intensities are seen. These factors indicate that more accurate information is available for computer processing. Data from this micrograph were used in the computer reconstructions shown in Fig. 8b and c.*

techniques revealed the truest image of the array, since migration of the negative stain is minimized by this method (42). However, in general, the changes between the low-dose and high-dose filtered reconstructed image were relatively minor, indicating that the negatively stained array is a comparatively beam-stable structure. This observation also indicated that routine microscopy provided a fairly accurate view of those elements that are already visible without the aid of spatial averaging techniques. It should be emphasized, however, that the spatial averaging technique revealed information about possible connecting structures between the rings that were not visible in an unprocessed micrograph and also revealed the morphology of the subunits within the rings.

Protein analysis of the isolated array.

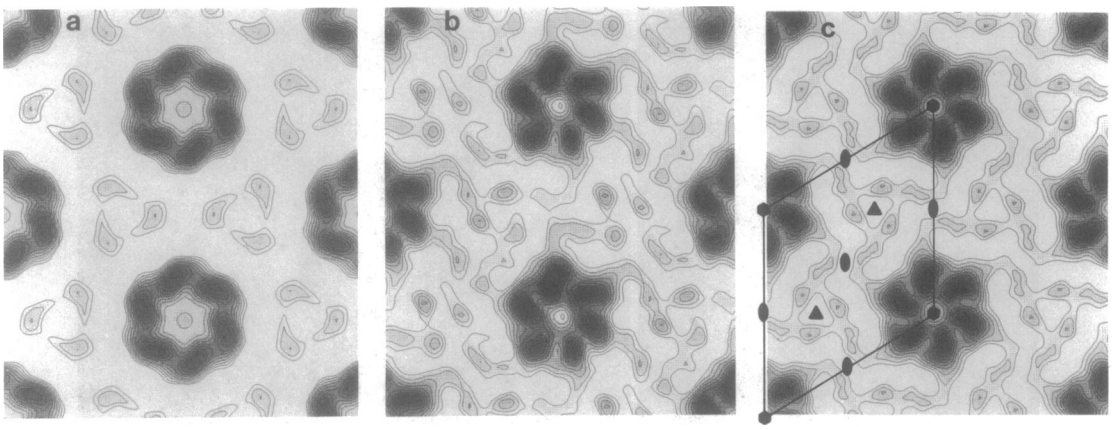

FIG. 8. *Superimposed gray scale and contour plots of spatially averaged images from micrographs taken under conditions of normal (high) and minimal (low) electron dose. In this representation, darker regions correspond to areas of greater stain exclusion, which is a reverse of contrast from negatively stained images. Center-to-center spacing between the dark rings is 23.5 nm. The minimum contour level was chosen subjectively to emphasize connectivity and does not imply protein boundaries. (a) A translationally and rotationally averaged high-electron-dose image. Data from Fig. 2 and another image were combined to produce this plot. (b) A translational average of Fig. 7 (a low-electron-dose image). The departures from p6 symmetry can be assessed visually as an adjunct to numerical measures of the discrepancy from symmetry. (c) A translationally and rotationally averaged low-dose image. Symmetrized data from Fig. 7, together with data from another ordered area on the same micrograph, were used. A single unit cell has been outlined, and the locations of the twofold (●), threefold (▲), and sixfold (⬢) rotational symmetry axes are indicated.*

The protein composition of isolated surface array preparations was analyzed by sodium dodecyl sulfate-polyacrylamide gel electrophoresis (Fig. 9). The majority of the protein was accounted for by polypeptides of 130,000 (130K), 74K, and 20K apparent molecular weights. Several other proteins were represented in reproducible but lesser amounts. Although a few flagella are present in the preparations, there was generally not enough to produce a band in the 25K region, where the major flagellin subunit protein migrates (19). The protein compositions of array materials from both 15NY106 and CB15 were identical, indicating that the ease in obtaining large arrays that were relatively free of intact outer membrane sheets in 15NY106 was not due to a major change in protein composition.

Some outer membrane material appeared to be present in all array preparations; hence, the question of which of the proteins revealed by gel electrophoresis actually form the array structures and which are integral membrane proteins must be approached with some caution. Thus far, we have been unable to separate the regular repeated structure from adherent membrane by using guanidine hydrochloride treatment, as was reported for *S. serpens* (9). Instead, only a partial solubilization of the component proteins has been effected in various attempts. The 130K protein is the predominant protein found in the cell; at any time in the cell cycle approximately 7% of the ^{14}C-amino acids incorporated into cellular protein is found in this peptide (data not shown). Outer membrane material, isolated by sucrose density gradient centrifugation, contains very little 130K proteins (3). Moreover, in macroscopic debris that often forms in high-density cultures, large amounts of the 130K protein are present (data not shown). It seems probable then that the 130K protein is the main component of the surface layer and that much of the periodic surface layer is lost from the outer membrane during preparation procedures. The 20K protein is also likely to be a component of the surface array, since it too is not represented in sucrose gradient-isolated outer membrane preparations (3).

The location of the 74K protein is more difficult to assess, but is also thought to be located in the superficial array structure because of its partitioning characteristics in isolation procedures. It was found at reproducible levels in array preparations; when 15NY106 and CB15 were compared (Fig. 3), quantitative densitometry always showed a precise 2:1 ratio of the 130K to the 74K protein in both preparations (data not shown), in spite of the fact that CB15 preparations appeared to contain more outer membrane material as intact sheets rather than as vesicles. The 74K protein is also a major protein in isolated outer membrane preparations (2, 3) and is present in levels comparable to a number of peptides that migrate between 74K and 130K proteins (2, 3). However, in the array

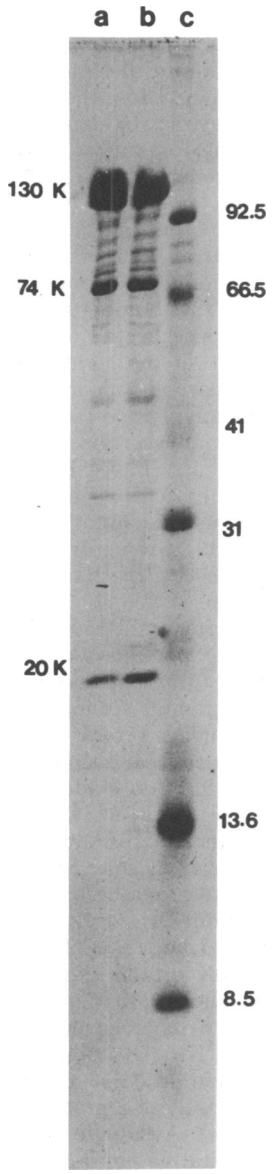

FIG. 9. *Sodium dodecyl sulfate-polyacrylamide gel electrophoresis of isolated surface array proteins. Lane a, Array isolated from strain 15NY106, which was largely free of underlying sheets of intact outer membrane material, but had abundant quantities of outer membrane vesicles. Lane b, Array isolated from the parent strain CB15. This latter preparation contained significant amounts of intact membrane material (Fig. 3). Note that the amounts of all proteins are similar in both preparation. The proteins discussed in the text are identified, but the minor species, which are not discussed, are also reproducibly found in all preparations. Lane c, Molecular weight standards: phosphorylase b (92.5K), bovine serum albumin (66.5K), alcohol dehydrogenase (41K), DNase I (31K), RNase A (13.6K) and ubiquitin (8.5K).*

preparations, 74K is a far more dominant species (Fig. 9) relative to those larger polypeptides. This suggests that 74K protein adheres more strongly to the outer membrane than does 20K or 130K protein, but is nevertheless a surface array protein. This logic also implies that several or all of the minor proteins migrating between 74K and 130K proteins may be outer membrane proteins. The above interpretation must remain tentative, however, as other explanations are possible. For example, it could be that 74K is indeed an integral outer membrane protein which attaches to surface array components. As such, it could well be uniformly enriched in array preparations, without having any role in the structure of the array.

DISCUSSION

A description of a surface array structure has not been previously published for *Caulobacter* species, despite the fact that this organism has been studied extensively, both morphologically and biochemically. The reason for this became obvious during the course of this investigation. The *Caulobacter* surface array was completely invisible by standard methods for fixing and staining of cells. It could not be determined with certainty whether the array was completely disrupted by fixation procedures lacking tannic acid or whether it was simply not stained by the heavy metal salts. There was no evidence of any organized elements remaining on the surface or present in the surrounding medium, and in light of the destructive effects of many negative stains on the array, we prefer the former explanation. Studies with *S. metamorphum* (6), in which the surface array may be visualized by the use of tannic acid, suggested the use of this component. In contrast to the partial success obtained in *S. metamorphum*, the appearance of the *Caulobacter* array was significantly stabilized by this treatment; all of the *Caulobacter* cells in each preparation showed a continuous and uniform layer of surface array.

Parenthetically, these results with tannic acid fixation point out once again the basic limitation of the use of electron microscopy as the sole criterion of purity for an isolation procedure in an otherwise uncharacterized system. As yet another example, examination by electron microscopy of a concentrated array preparation using uranyl acetate as negative stain indicated only a relatively pure preparation of the few flagella that remained in the sample, since they are unaffected by the stain.

The *Caulobacter* surface array is a structure of unusual complexity and has features that both distinguish and correlate this layer with the

surface arrays of other bacteria. The periodic components of the surface layer display p6 planar symmetry with a six-subunit ring structure. The size of the six-membered ring is similar to that found in *S. serpens* and several other organisms (13, 31). The instability at low pH, the presence of a high-molecular-weight protein as a major component, and the beneficial fixation effects of tannic acid are also features common to other surface arrays (6–8, 9, 10, 14, 17, 30). The stabilization effects of divalent cations and the observation that quantities of intact array are sloughed off the cells have also been reported in other systems (7, 8, 31). The *Caulobacter* surface array was dissimilar to other array systems in the large distance found between the repeating units and the evidence of being a multipeptide complex (31).

The optical diffraction and computer processing data indicated that the rings, although not directly attached to one another, are positioned with a high degree of precision, both in the unit spacing (or lattice constant) and in the absence of rotational freedom of the subunits within the ring. Thus, structural elements must be present between the rings, although no connecting structures were revealed by freeze-etching or in the unprocessed, perpendicular views of negatively stained array patches. For freeze-ethching, this is explained by the lower resolving capabilities of the technique. In perpendicularly viewed negative-stained specimens, the absence of interconnecting structure was probably due to a high ratio of entrained stain relative to the size of the interconnecting elements. Interconnecting structural elements were only poorly resolved by thin-sectioning and edge views of negatively stained membrane vesicles with attached surface array.

The 130K protein, which is the most abundant of the proteins seen in the array material, has a pI of 4.6 as determined by two-dimensional gel electrophoresis (M. Milhausen and N. Agabian, manuscript in preparation). The large size or acidic nature, and often both, are properties common to the major proteins in a number of bacterial surface arrays including *Clostridium* sp. (30), *Bacillus sphaericus* (17), and *Acinetobacter* sp. (39). In these bacteria, this type of protein forms the highly visible unit that is responsible for strong reflections in optical diffraction analysis. It may be that the 130K protein forms the individual subunits of the six-member ring in the *Caulobacter* array. However, in most of the above organisms, the repeated units form a closely packed structure, and the protein contained in the units is the only species present in the layer. In contrast, the *Caulobacter* array may well have a number of peptides, and there is a considerable space between units, likely requiring additional linking molecules to maintain the precise arrangement as discussed above. Thus, the structure of the *Caulobacter* array may be significantly different from that of other organisms, making assumptions based on general features of bacterial arrays impossible.

There are also other limitations at this stage of the surface array analysis. Although there appear to be a number of polypeptides in the structure, their exact number is not known. It is also not known whether all of the linking elements are visible in the computer reconstructions. Since the correspondence between visible structures and polypeptide components cannot be made, we cannot ascertain whether all of the structural elements have been catalogued. Therefore, the physical, visual, and computer averaging information cannot be unequivocally compared, and the true nature and complexity of the interconnecting mechanisms must await further resolution.

The surface array of CB15 having been characterized, it was possible to determine that CB13, the other *Caulobacter* strain commonly used in developmental studies, has no visible evidence of an array. Freeze-etching, negative staining of whole cells, and thin-sectioning with tannic acid provided no evidence of a regular surface structure (data not shown). However, there was some indication that certain elements or vestiges of an array may be present in this strain. For example, material can be pelleted by centrifugation from CB13 culture supernatants that is greatly enriched for a 22K protein similar in size to the 20K protein described for strain CB15 (data not shown). In high-density cultures of both strains, a macroscopic, fibrous debris often forms. In CB15, this debris is almost entirely 130K protein. In CB13, the debris is composed almost entirely of a protein of about 75K (data not shown). Although differing in size, other less quantitative characteristics, such as detergent solubility and a characteristic streaked migration pattern in sodium dodecyl sulfate-polyacrylamide gel electrophoresis, are also shared by these two proteins. It seems possible that CB13 has lost some elements of a surface array while retaining others. In support of this possibility is the 1967 report of Poindexter et al. (25) that the CB13 membranes contained "cell wall subunits." Although not identified as part of a regular surface structure, there are indications that these subunits were regularly aligned (J. Poindexter, personal communication). Since both strains have been in laboratory culture for many years, it may be that the absence of an environmental stress has resulted in the disap-

pearance of the structure in CB13. Examination of culture collections may resolve this point.

The function of the *Caulobacter* surface array is unknown. In some bacteria, such as *B. sphaericus,* intensive efforts to isolate strains devoid of the structure have failed (17), suggesting that the presence of the layer is mandatory. In other genera, such as *Spirillum* (31), presence of an organized layer may be optional, since some strains have one, and others do not. The genus *Caulobacter* appears to be of this latter type.

Recent work with other bacterial species has led to the proposal that their surface layers may represent a physical barrier to large "unfriendly" molecules, presenting only 2- to 3-nm holes in the cell surface (35, 36). Although the *Caulobacter* array also appears to have a hole of similar dimensions in its repetitive unit, the large spacing between the units argues against an analogous barrier role.

This surface array may present an excellent system for studying questions concerning the mechanisms of membrane protein insertion and membrane biogenesis. The proteins involved are produced in larger amounts than any other class of proteins in the cell and are translated from a family of stable mRNA's (2). This information and the ability to readily isolate the array in biochemically significant quantities permit many approaches to the purification of individual proteins and facilitate their physical characterization and the eventual study of their regulation of expression. The fact that these membrane proteins form structures that are distinguishable by visual techniques provides an assay not available to most membrane systems studied. For example, it should be possible to localize the proteins to specific structural elements of the array by specific-antibody labeling techniques. Using recently developed methods, it is possible to treat a specimen with an antibody directed to individual proteins and determine the average binding position by using spatial averaging techniques, such as those described in this study (1). The highly ordered structure, high-beam stability, and ability to work with the large areas of material make the *Caulobacter* surface array especially amenable to such a study. *C. crescentus* also provides a system for the study of complex events in membrane structure and function. The cellular stalk of this organism has been thought to be biochemically inert, since the internal region contains no ribosomes and appears to be isolated from the remainder of the cell by an ill-defined "plug" at the base of the stalk (24). Yet we noted that the surface array also extends over the entire stalk (Fig. 1). An understanding of how the array arrives at this location could reveal mechanisms of both membrane biogenesis and the formation of this membrane structure.

ACKNOWLEDGMENTS

We thank Hiroshi Nikaido and Linda Thomashow for helpful comments during the preparation of this manuscript. We also thank James Lara for his generous cooperation in the use of the JEOL 100B electron microscope and James Koehler for the use of the freeze-fracture apparatus.

This research was supported at the University of Washington by Public Health Service grants GM 25527 (N.A.) and AI 05946 (J.S.) from the National Institutes of Health. The work at the University of California, Berkeley, was supported by Department of Energy Contract W-7405-eng-48 and National Institutes of Health research grant GM 23325.

LITERATURE CITED

1. **Aebi, U., B. Ten Heggeler, L. Oronato, J. Kistler, and M. K. Showe.** 1977. New method for localizing proteins in periodic structures: Fab fragment labeling combined with image processing of electron micrographs. Proc. Natl. Acad. Sci. U.S.A. **74**:5514–5518.
2. **Agabian, N., M. Evinger, and G. Parker.** 1979. Generation of asymmetry during development. J. Cell Biol. **81**:123–136.
3. **Agabian, N., and B. Unger.** 1978. *Caulobacter crescentus:* effect on murein and outer membrane protein composition. J. Bacteriol. **133**:987–994.
4. **Agabian-Keshishian, N., and L. Shapiro.** 1971. Bacterial differentiation and phage infection. Virology **44**: 46–53.
5. **Baumeister, W., and O. Kübler.** 1978. Topographic study of the cell surface of *Micrococcus radiodurans.* Proc. Natl. Acad. Sci. U.S.A. **75**:5525–5528.
6. **Beveridge, T. J., and R. G. E. Murray.** 1975. Surface arrays on the cell wall of *Spirillum metamorphum.* J. Bacteriol. **124**:1529–1544.
7. **Beveridge, T. J., and R. G. E. Murray.** 1976. Reassembly *in vitro* of the superficial cell wall components of *Spirillum putridiconchylium.* J. Ultrastruct. Res. **55**: 105–118.
8. **Beveridge, T. J., and R. G. E. Murray.** 1976. Superficial cell-wall layers on *Spirillum* "Ordal" and their *in vitro* reassembly. Can. J. Microbiol. **22**:567–582.
9. **Buckmire, F. L. A., and R. G. E. Murray.** 1970. Studies on the cell wall of *Spirillum serpens.* I. Isolation and partial purification of the outer most cell wall layer. Can. J. Microbiol. **16**:1011–1022.
10. **Buckmire, F. L. A., and R. G. E. Murray.** 1973. Studies on the cell wall of *Spirillum serpens.* II. Chemical characterization of the outer structural layer. Can. J. Microbiol. **19**:59–66.
11. **Chester, I. R., and R. G. E. Murray.** 1978. Protein-lipid-lipopolysaccharide association in the superficial layer of *Spirillum serpens* cell walls. J. Bacteriol. **133**:932–941.
12. **Cohen-Bazire, G., W. R. Sistrom, and R. Y. Stanier.** 1957. Kinetic studies of pigment synthesis by non-sulfur purple bacteria. J. Cell. Comp. Physiol. **49**:25–68.
13. **Glaeser, R. M., W. Chiu, and D. Grano.** 1979. Structures of the surface layer of the outer membrane of *Spirillum serpens.* J. Ultrastruct. Res. **66**:235–242.
14. **Glauert, A., and M. J. Thornley.** 1969. The topography of the bacterial cell wall. Annu. Rev. Microbiol. **23**:159–198.
15. **Hollaus, F., and U. Sleytr.** 1972. On the taxonomy and fine structure of some hyperthermophilic saccharolytic clostridia. Arch. Mikrobiol. **86**:129–146.
16. **Horne, R. W., and I. P. Ronchetti.** 1974. A negative staining-carbon film technique for studying viruses in the electron microscope. J. Ultrastruct. Res. **47**:361–383.
17. **Howard, L., and D. J. Tipper.** 1973. A polypeptide

bacteriophage receptor: modified cell wall protein subunits in bacteriophage-resistant mutants of *Bacillus sphaericus* strain P-1. J. Bacteriol. **113**:1491–1504.

18. **Laemmli, U. K.** 1970. Cleavage of structural proteins during the assembly of the head of bacteriophage T4. Nature (London) **227**:680–685.
19. **Lagenaur, C., and N. Agabian.** 1976. Physical characterization of *Caulobacter crescentus* flagella. J. Bacteriol. **128**:435–444.
20. **Muller, L. L., and T. J. Jacks.** 1975. Rapid chemical dehydration of samples for electron microscopic examination. J. Histochem. Cytochem. **23**:107–110.
21. **Nermut, M. V., and R. G. E. Murray.** 1967. Ultrastructure of the cell wall of *Bacillus polymyxa*. J. Bacteriol. **93**:1949–1965.
22. **Poindexter, J. S.** 1964. Biological properties and classification of the *Caulobacter* group. Bacteriol. Rev. **28**: 231–295.
23. **Poindexter, J. S.** 1978. Selection for nonbuoyant morphological mutants of *Caulobacter crescentus*. J. Bacteriol. **135**:1141–1145.
24. **Poindexter, J. S., and G. Cohen-Bazire.** 1964. The fine structure of stalked bacteria belonging to the family of Caulobacteraceae. J. Cell Biol. **23**:587–607.
25. **Poindexter, J. S., P. R. Hornack, and P. A. Armstrong.** 1967. Intracellular development of a large DNA bacteriophage lytic for *Caulobacter crescentus*. Arch. Mikrobiol. **59**:237–246.
26. **Ridgway, H. F., R. M. Wagner, W. T. Dawsey, and R. A. Lewin.** 1975. Fine structure of the cell envelope layers of *Flexibacter polymorphus*. Can. J. Microbiol. **21**:1733–1750.
27. **Shapiro, L.** 1976. Differentiation in the *Caulobacter* cell cycle. Annu. Rev. Microbiol. **30**:377–407.
28. **Shapiro, L., N. Agabian-Keshishian, A. Hirsch, and O. M. Rosen.** 1972. Effect of dibutyryladenosine 3′5′-cyclic monophosphate on growth and differentiation in *Caulobacter crescentus*. Proc. Natl. Acad. Sci. U.S.A. **69**:1225–1229.
29. **Simionescu, N., and M. Simionescu.** 1976. Galloylglucose of low molecular weight as mordant in electron microscopy. J. Cell Biol. **70**:608–621.
30. **Sleytr, U. B.** 1975. Heterologous reattachment of regular arrays of glycoprotein on bacterial surfaces. Nature (London) **257**:400–402.
31. **Sleytr, U. B.** 1978. Regular arrays of macromolecules on bacterial cell walls: structure, chemistry, assembly and function. Int. Rev. Cytol. **53**:1–64.
32. **Sleytr, U. B., and A. M. Glauert.** 1976. Ultrastructure of the cell walls of two closely related clostridia that possess different regular arrays of surface subunits. J. Bacteriol. **126**:869–882.
33. **Smit, J., and H. Nikaido.** 1978. Outer membrane of gram-negative bacteria. XVII. Electron microscopic studies on porin insertion sites and growth of cell surfaces of *Salmonella typhimurium*. J. Bacteriol. **135**: 687–702.
34. **Southworth, D., K. Fisher, and D. Branton.** 1975. Principles of freeze-fracturing and etching, p. 247–282. *In* D. Glick and R. Rosenbaum (ed.), Techniques of biochemical and biophysical morphology, vol. 2. John Wiley & Sons, Inc., New York.
35. **Stewart, M., and T. J. Beveridge.** 1980. Structure of the regular surface layer of *Sporosarcina urea*. J. Bacteriol. **142**:302–309.
36. **Stewart, M., T. J. Beveridge, and R. G. E. Murray.** 1980. Structure of the regular surface layer of *Spirillum putridiconchylium*. J. Mol. Biol. **137**:1–8.
37. **Taylor, K. A., and R. M. Glaeser.** 1973. Hydrophilic support films of controlled thickness and composition. Rev. Sci. Instrum. **44**:1546–1547.
38. **Thorne, K. J. I., R. C. Oliver, and M. F. Heath.** 1976. Phospholipase A_2 activity of the regularly arranged surface protein of *Acinetobacter* sp. 199A. Biochim. Biophys. Acta **450**:335–341.
39. **Thornley, M. J., K. J. I. Thorne, and A. M. Glauert.** 1974. Detachment and chemical characterization of the regularly arranged subunits from the surface of an *Acinetobacter*. J. Bacteriol. **118**:654–662.
40. **Watson, S. W., and C. C. Remsen.** 1970. Cell envelope of *Nitrosocystis oceanus*. J. Ultrastruct. Res. **33**:148–160.
41. **West, D. C., C. Lagenaur, and N. Agabian.** 1976. Isolation and characterization of *Caulobacter crescentus* bacteriophage φCd1. J. Virol. **17**:568–575.
42. **Williams, R. C., and H. W. Fisher.** 1970. Electron microscopy of tobacco mosaic virus under conditions of minimal beam exposure. J. Mol. Biol. **52**:121–123.